Computational analysis of room pressure control in airtight cleanrooms

Rick Kramer*[1], Raymon Wasman[1], Frans Saurwalt[2], Derek Vissers[2], and Marcel Loomans[1]

[1] *Eindhoven University of Technology*
De Zaale
Eindhoven, the Netherlands
**Corresponding author: r.p.kramer@tue.nl*

[2] *Kropman Installatietechniek*
Lagelandseweg 84
Nijmegen, the Netherlands

ABSTRACT

Room pressure differential is an important aspect in order to guarantee sufficient contamination control, but is difficult to control in airtight cleanrooms. This research uses simulation models to get an understanding and to quantify the room pressure controllability of airtight cleanrooms. The most influential parameters on the room pressure controllability are identified using a sensitivity analysis. The effects of the shell airtightness and overflow flowrates are quantified, and the effect of a flow/pressure cascade with three coupled rooms is investigated. Also, the effect of other parameters in the control system on the room pressure controllability are quantified. The main conclusion is that creating a flow/pressure cascade with a substantial flow rate can lead to significant improvements in room pressure controllability.

KEYWORDS

Cleanroom, airtightness, pressure, control, energy

1 INTRODUCTION

Contamination control in cleanrooms is essential in many disciplines. For example, for the semiconductor industry, contamination must be kept outside the cleanroom, while for pharmaceutical research or vaccine production involving viruses, the contamination (the virus) must be kept inside to prevent spreading. The cleanroom is separated from adjacent rooms by a shell (walls, floor, ceiling), however, this shell is not entirely airtight. Therefore, a flow/pressure cascade is created between the cleanroom and its surroundings to prevent contamination to enter or leave the cleanroom. A sufficiently over-pressured cleanroom will result in a flow from the cleanroom to adjacent rooms, and vice versa in the case of an under-pressured cleanroom.

The over- or under-pressure is created by a difference between the mechanically supplied and extracted air volume flow, the so-called offset. A higher offset results in a higher airflow through the shell and a higher pressure over the shell. The airtightness of cleanroom shells has been improved over the past decades for better contamination control and to save energy, i.e. by reducing the leakage volume flow (ISO, 2019) (ISO, 2021). An air tighter shell results in a higher pressure difference with the same offset, or a lower offset for the same pressure difference. High over- or under-pressures in cleanrooms can have negative effects such as high velocities through cracks leading to noise and opening doors can become difficult (R&D world online, 2012). Therefore, in practice the room pressure difference setpoint is maintained at a regular level while the offset is reduced. The recommended pressure difference for cleanrooms with different cleanliness levels varies from 7.5 Pa to15.0 Pa (ISO, 2021). However, a small

offset hinders a robust control of the cleanroom pressure differential, because small variations in the offset result in a larger change of room pressure than in rooms with a large offset. The room pressure also becomes harder to control with smaller cleanrooms and for cleanrooms with higher air change rates (Saurwalt, 2018). Practice shows that sometimes the room pressure differential control cannot be realized sufficiently accurate, and that extra holes are made in the shell to decrease the airtightness of the room (ABN Cleanroom Technology, 2020).

Earlier research has investigated methods how to improve room pressure control, such as (van den Brink & van Schijndel, 2012). These studies focus on situations with external disturbances, such as opening a door. No research could be found which investigates imperfections of the room pressure control system and internal disturbances, which for an airtight cleanroom can already make the room pressure control very difficult. Imperfections and internal disturbances of the room pressure control include factors like sensor inaccuracies, pre-pressure fluctuations, reference pressure fluctuations, delays, runtimes, backlash, and resolution of actuators and sample times of sensors and controllers. To effectively benefit from airtight cleanrooms in terms of energy-efficiency and contamination control, this research investigated which internal system and control factors influence the room pressure control the most and how these factors can be influenced to increase the controllability of cleanroom pressure control.

2 METHODOLOGY

2.1 Simulation model

Matlab Simulink has been used to for modelling and dynamic simulations. The basis of the model is a mass balance of the air mass inside the room over time. The mass in the room depends on the difference between entering air (supply + leakage airflow + incoming overflow if under-pressure) and leaving air (exhaust + leakage airflow + outgoing overflow if over-pressure) and was calculated over time, according to

$$m(t) = \int_{t=0}^{t_{end}} \dot{m}_{incoming}(t) - \dot{m}_{extracted}(t)\, dt \quad (1)$$

The air pressure in the room was calculated using the ideal gas law, according to

$$P(t) = \frac{m(t)*R*T}{V} \quad (2)$$

Where *m(t)* is the mass of the air in the room at time *t*, *R* is the gas constant of air, *T* is the room air temperature and *V* is the room volume. The ideal gas law assumes a homogeneous pressure throughout the room.

Airflow caused by leakage through the shell was calculated according to (VCCN, 2018),

$$Q(t) = f * \Delta P(t)^n \quad (3)$$

Where *f* is the leakage factor of the shell, *ΔP* is the pressure difference over the shell part, and *n* is the flow exponent. The leakage factor and flow exponent are properties of the shell and can be determined with an airtightness test of the cleanroom. Overflow was calculated similarly to Equation (3).
The HVAC system of a cleanroom contains multiple dampers to maintain a certain ventilation rate using VAVs and to maintain the room pressure setpoint using control dampers. The flowrate through a damper was determined, assuming a damper position of 45˚ at nominal flow rate, according to,

$$Q\ (t) = Q_{nom} * \sqrt{\frac{\Delta P_{at\ Qnom}}{\Delta P_{at\ current\ valve\ position}(t)}} \quad (4)$$

Where $\Delta P_{at\ Qnom}$ is the pressure loss at nominal airflow, and $\Delta P_{at\ current\ valve\ position}(t)$ is the pressure loss with the damper position at time *t*.

The pressure loss over the damper was calculated according to (Ti-soft, 2017),

$$\Delta P(t) = 0.5 * \rho * \zeta(t) * v(t)^2 \quad (5)$$

Where ζ is the pressure drop coefficient, which depends on the damper position, and *v* is the air velocity through the damper at time *t*. The pressure loss of the duct system was calculated by the Colebrook-White equation and the Darcy-Weisbach equation. The pressure loss over the HEPA filter was modeled using a linear relationship with the flowrate (Xu, 2014), based on the initial pressure drop provided by the manufacturer at the design flow rate of the filter.
Additionally, the flowrate through a damper is influenced by the total pressure difference between both sides of the duct, which is the room on one side, and the AHU head on the other side, which has been calculated according to,

$$mf = \sqrt{\frac{\Delta P_{current}(t)}{\Delta P_{nominal}}} \quad (6)$$

Where *mf* is the resulting multiplication factor for the flow through the damper, $\Delta P_{nominal}$ is the nominal absolute pressure difference between the AHU head and the room, and $\Delta P_{current}(t)$ is the current pressure difference between the AHU head and the room.

It is common that air duct designs include two or more parallel dampers: A duct splits up into multiple branches including dampers, and then converges back into a single duct. If one damper closes, the pressure will rise, causing more air to flow through the other parallel dampers. In the simulation model, parallel dampers are treated as separate systems, but the pressure drop of the duct and filters were equal to the design flow fraction through each parallel damper.

The inaccuracy of the flow rate sensor in the VAV unit was modelled as follows. Based on the inaccuracy provided in the product specification sheet, a uniformly distributed number within the inaccuracy range was generated at a certain time interval and added to the flow rate reading of the VAV unit.

The controller of the damper that controls the room pressure does not use the reading of the flow rate, but uses the reading of the room pressure sensor. The three most significant factors that contribute to the inaccuracy of a room pressure sensor are hysteresis, non-repeatability, and non-linearity (Gassmann, 2014). Hysteresis was modeled using the Simulink backlash block. Non-repeatability was modeled using a randomly uniformly distributed number generator, of which the outcome was added to the sensor reading value. Although non-linearity is an important factor in sensor accuracy, it was not model, because it is a unique characteristic for every sensor, which is unknown. Zero-point error and span error have not been modeled, as those errors can be fixed during the calibration process (Instrumentationtools.com, n.d.).

The resolution of the actuator, i.e. the number of steps the rotating scale of the actuator is divided into, has been modelled. Also, the run time of the actuator (the time from 0° to 90°

position) has been modelled. The actuator and damper linkage combination is subjected to backlash which has been modeled with the Simulink backlash block as 1% (Belimo, 2020).

2.2 Case study

A real-life case study was used as a starting point to work with real values, proportions, and HVAC design: A biosafety laboratory where research on polio vaccines is performed. The laboratory is newly built in an already existing building and is operational since the start of 2022. The cleanroom has an under-pressure of -45 Pa relative to the atmosphere. The room has a door without airlock to the corridor, where the design pressure is -30 Pa. The design shell airtightness is VCCN RL 10 level 2.5 (leakage factor 0.006 $(l/s.m^2)/Pa^{0.65}$) on a scale from L0 to L5. The leakage test measurement revealed that the leakage factor in reality is lower (0.005048 $l/s.m^2)/Pa^n$), but the flow exponent *n* is higher (0.75 instead of the default 0.65).
The volume of the room is 154 m^3 and the air change rate is 15.3 h^{-1}. Air is supplied to the room with a flowrate of 2,350 m^3/h and is controlled by two parallel VAV units. Air is extracted from the room by (i) two biosafety cabinets (BSC) of which each extracts 600 m^3/h and has its own duct and VAV unit, and (ii) lower returns in the wall connecting to one duct which leads to three parallel dampers including one VAV and two control dampers for room pressure control. The design states that 850 m^3/h flows through the VAV and 200 m^3/h flows through each control damper. These airflow rates imply an offset of 100 m^3/h of which 50 m^3/h enters the room via an adjustable door sill located in the door to the corridor. The other 50 m^3/h enters the room via the shell leakage. The room leakage test results show that the shell leakage is higher than in the design, i.e. 70.3 m^3/h, which results in a total offset of 120.3 m^3/h. This value is used in the simulations. The full parameter data set of the case study that is used for the simulation model is not included for brevity.

2.3 Calibration

BMS data was used to calibrate the disturbance amplitudes and characteristics of the model. The first disturbance is pre- and suction-pressures: A sine wave with given amplitude and period was used superposed to a random number (within given range). The second disturbance is the variation of the room pressure in the corridor which is important because the room pressure is controlled relative to this corridor and pressure fluctuations in the corridor have an effect on the airflow into the room via the door sill. This disturbance is modeled by superposing three sine waves, with different amplitude and period, based on the BMS data. The third and last disturbance is the VAV airflow sensor inaccuracy for which max. 3% was used in the random number generator.

The pressure control accuracy of the case study and of the simulation model were quantified: Both the simulated room pressure and the measured room pressure were compared to the pressure setpoint using three criteria: (i) The Mean Absolute Error (MAE), (ii) The Mean Squared Error (MSE), and (iii) Visually comparing the room pressures over time.

2.4 Sensitivity analysis

The sensitivity analysis was performed using 11 parameters. From each of those parameters, a range was selected from 40% below the nominal value to 40% above the nominal value. The nominal value is the value used in the simulation model after the calibration process. The sensitivity analysis was executed using the Simulink sensitivity analyzer tool. Then, Monte Carlo-like simulations were performed for 1000 combinations of different parameter values. The sampling method used is Latin Hypercube sampling. Next, a standardized ranked regression analysis was performed to investigate both the magnitude of the influence of each

parameter and the direction of the relationship (positive or negative) based on the Mean Absolute Error (MAE), calculated according to

$$MAE = \frac{1}{t_{end}-30} \int_{t=30}^{t_{end}} \left| P_{setpoint} - P_{realized}(t) \right| dt \quad (7)$$

Initially, an energy balance was modeled to investigate the influence of supply air temperature fluctuations on the room pressure control. However, a preliminary analysis showed that temperature fluctuations have a negligible effect on the room pressure control.

3 RESULTS

3.1 Calibration

Only the VAV-sensor inaccuracy sampling time needed adjustment for the calibration. A sampling time of 5 s yielded the best results, see Table 1. The simulation differs 7.9% from the BMS data for both the MAE and MSE. Figure 1 compares room pressure over time between the case study data and the simulation data. For readability, the graph only shows a selection of the total available case data (30 minutes). Generally, the dynamics and amplitudes match.

Table 1 Calibration criteria

Criteria	BMS	Simulation	Error
MAE [Pa]	0.298	0.275	7.9%
MSE [Pa^2]	0.133	0.122	7.9%

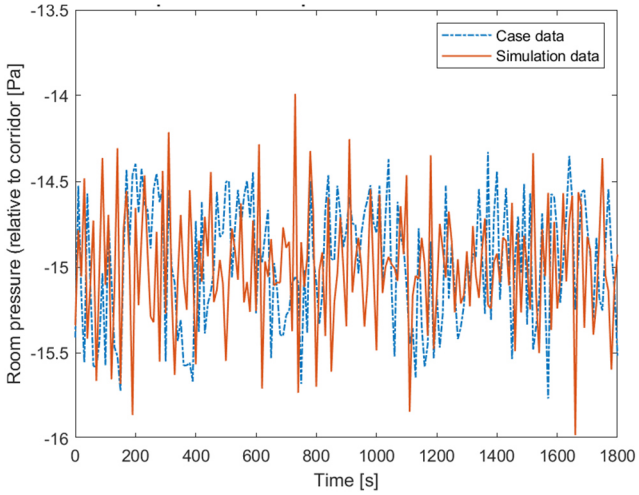

Figure 1. Room pressure comparison

3.2 Sensitivity analysis

Initially, the bypass fraction was included as a parameter. The results revealed that the bypass fraction has a major influence on the room pressure control, ranking in the top 2, and that the room pressure error decreases with a higher bypass factor. However, this parameter also caused major outliers in the sensitivity analysis, mostly occurring when the bypass factor was near its maximum value. This is probably caused by maintaining constant PID-controller settings and possibly also because there may be an optimum bypass fraction. Hence, the bypass factor was removed from the final sensitivity analysis to increase the reliability of the statistical analysis.

Figure 2 shows the results of the sensitivity analysis ranking the remaining 10 parameters. A higher score implies a higher influence of the parameter on the room pressure controllability. Besides the bypass factor, most influential are the control damper runtime, the overflow rate, control loop delay, room pressure setpoint and shell airtightness. The room pressure controllability is less influenced by the other parameters.

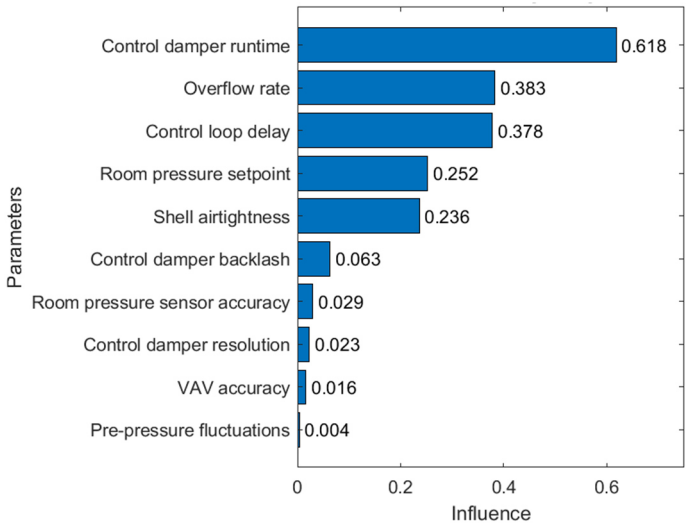

Figure 2. Results of the sensitivity analysis

3.3 Airtightness and overflow

To further investigate the influence of the shell airtightness and overflow on the room pressure controllability, more simulations were performed. Figure 3 shows the relation between the shell airtightness and the MAE of room pressure for four different overflow rates, ranging from 0 m^3/h to 200 m^3/h. In the simulations, the mechanical supply was maintained at a constant level, while the mechanical extraction depended on the leakage flow. The shell airtightness ranges from 0.000 to 0.081 $(l/s.m^2)/Pa^n$, with the latter being the least airtight class from the VCCN RL10 classification.

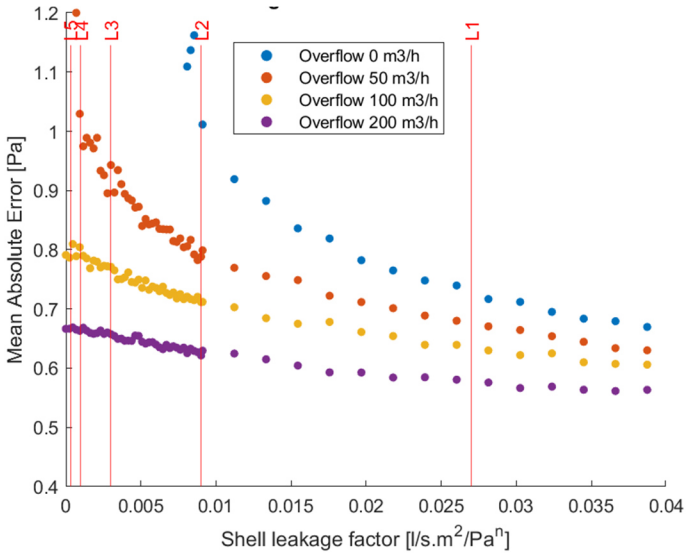

Figure 3. Shell airtightness and overflow versus the mean absolute room pressure error

The room pressure controllability appears to be better enhanced when the overflow rate is high and the airtightness is low, which is in line with theory. Moreover, the airtightness of a room becomes less critical when the overflow rate is higher regarding the room pressure controllability. When there is no leakage at all, i.e. no overflow and no leakage through the shell, the room pressure is uncontrollable and the MAE peaks at 15 Pa. While maintaining the overflow at zero, but reducing the shell airtightness, the controllability increases exponentially. This emphasizes the fact that some leakage is necessary in order to guarantee room pressure

controllability. For an overflow rate of 100 m^3/h, the MAE can be decreased by 7.7% by changing the room airtightness from VCCN Level 3 to Level 2. At an overflow rate of 200 m^3/h, decreasing the shell airtightness from Level 3 to Level 2 decreased the MAE by 5.5%.

3.4 Flow/pressure cascade

In a flow/pressure cascade design, air is supplied in one room and flows via one or more adjacent rooms to the last room in the cascade, where the air is extracted. The flow rate and direction are determined by the pressure difference between the rooms. The reference case only makes use of this principle to a very small extent as 50 m^3/h flows from the corridor through the door's sill into the cleanroom.

The simulation model was adapted to three connected room of which the properties are the same as the reference case room. The first room is connected to a non-pressure-controlled area at atmospheric pressure without pressure variation. The pressure of this first room is -15 Pa controlled relative to the atmospheric pressure. The second room has a room pressure of -30 Pa relative to the atmosphere, which is controlled relative to the first room at -15 Pa. The third room does have a pressure of -45 Pa relative to the atmosphere and its pressure is controlled relative to the second room at -15 Pa.

Two scenarios were simulated. In both scenarios, the overflow rate is increased with each simulation in steps of 50 m^3/h up to a total of 2,350 m^3/h. In the first scenario, the mechanical supply flow rate was maintained at 2,350 m^3/h (which is the original design flow rate), while the mechanical extraction was raised when the net overflow flowrate increased (incoming overflow – outgoing overflow) to balance the offset. In the second scenario, the total supplied flowrate was maintained at 2,450 m^3/h (i.e. the incoming overflow + the mechanical supply). This implies that when the incoming overflow increased, the mechanical supply decreased. The nominal extraction flowrate again is adjusted in such a way that the offset was balanced. Basically, the second scenario used supplied air multiple times for different rooms, which reducing the energy demand.

Figure 4 shows the results of the nominal overflow rate versus the MAE for both scenarios and for each of the three rooms in the flow/pressure cascade. The scenario that maintains a constant total supply flowrate (mechanical + incoming overflow) outperforms the scenario that only maintains a constant mechanical supply flowrate. Especially for increasing overflow rates, the difference in MAE between those scenarios increases. At an overflow rate of 2,350 m^3/h, the scenario with constant total supply flowrate achieves a 60% lower MAE than the scenario with constant mechanical supply. Interestingly, increasing the overflow rate in the scenario with constant mechanical supply does have a lower effect on the MAE reduction than in the scenario with constant total supply.

In both scenarios, the controllability is better for the rooms at the end of the flow/pressure cascade, i.e. the room at -45 Pa. It is clear that a flow/pressure cascade with substantial overflow rates can lead to significantly improved pressure controllability compared to the reference situation.

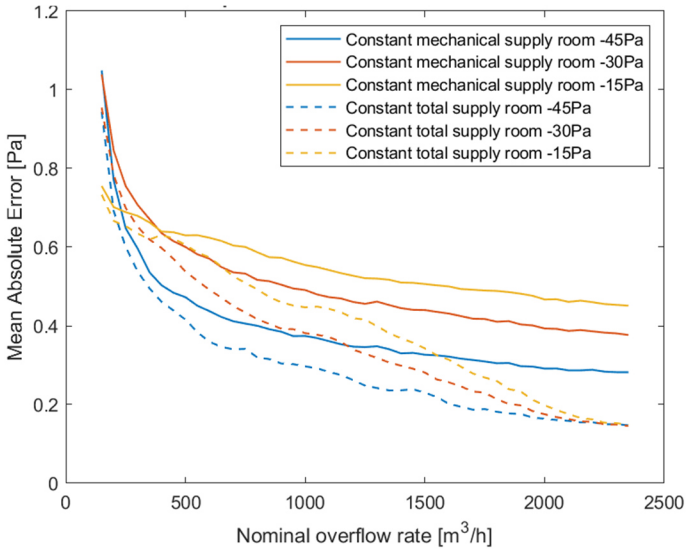

Figure 4. MAE of the room pressure control using a flow/pressure cascade

3.5 Bypass fraction

The bypass fraction is the nominal flow rate through the bypass divided by the total mechanical exhaust flow rate. Although the bypass fraction was not used as a parameter in the Monte-Carlo-like sensitivity analysis combining different parameter values, it has been investigated in an individual sensitivity analysis by varying only the bypass fraction in the simulation model. The original value in the case was 16.3%.

Figure 5 shows that the MAE, the measure for the room pressure controllability, decreases by increasing the bypass fraction up to 12%. For bypass fractions higher than 12%, there is no significant effect on the MAE. For bypass fractions lower than 12%, the control damper lacks authority on the flow rate at all times (not shown): The control dampers reach their maximum positions many times while room pressure setpoint was not achieved. This means that the control damper in this situation cannot sufficiently manipulate the exhaust airflow, meaning the offset does not match with the leakage flow, resulting in severe pressure fluctuations. Therefore, it is important to use a sufficiently large bypass fraction to be able to control the room pressure accurately.

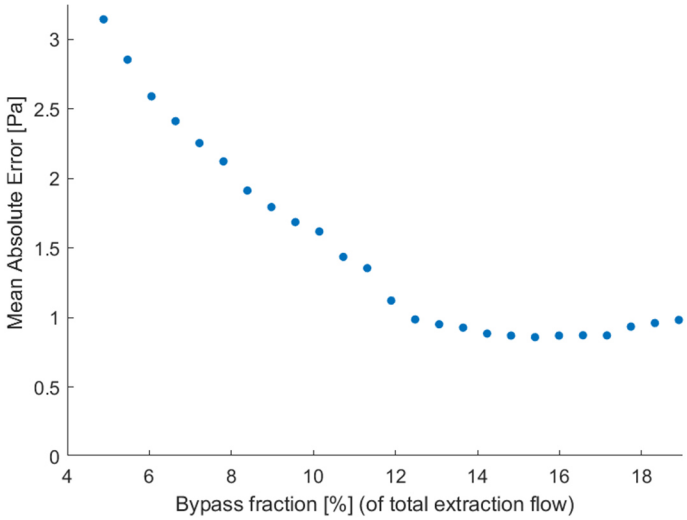

Figure 5. Bypass fraction versus the mean absolute room pressure error

3.6 Sensor damping and controller dead band

In the control system, there are two software components affecting the control system behavior that are incorporated on purpose. Firstly, a damping factor in the room pressure sensor to reduce quickly varying room pressure readings. Hence, the controller receives a smoother signal for room pressure reducing the actuator movement. A simulation was conducted with and without room pressure sensor damping. The simulation with the damping activated (which is the original case situation) resulted in a MAE of 0.879 Pa. Without damping factor, the MAE was reduced to 0.562, i.e. a reduction of 35.2%, but the damper actuators moved 19.0% more (total rotation angle).

Secondly, a dead band around the room pressure setpoint is used for less actuator movement and help reduce oscillations (Wishart, 2018). In the reference case, this dead band was 0.5 Pa, i.e. if the measured room pressure is within -15.5 and -14.5 Pa (setpoint = -15 Pa), the controller output is maintained at a constant level and the actuator does not move. When the dead band is removed from the controller, the MAE reduces to 0.703 Pa, i.e. a reduction of 20.1%. Interestingly, the simulation shows that the movement of the damper actuator (total rotation angle) is reduced by 28.1% in comparison to the original situation.

4 DISCUSSION AND CONCLUSIONS

This research employed simulation models to get an understanding and to quantify the room pressure controllability of airtight cleanrooms. The most influential parameters on the room pressure controllability have been identified using a sensitivity analysis. The limitations of this study are mostly related to uncertainty in modelling. For example, modeling of the VAV inaccuracy is simplified, because of a lack of information, using a certain inaccuracy value and a random number generator that picks a number within the given inaccuracy range every 5 seconds. Hence, it is recommended to address the inaccuracy modeling of VAV units in future research.
Another limitation is the fact that the PID-controller settings are kept constant throughout the research, and hence, parameters that determine the controller settings (such as runtime, delays times, and bypass fraction) most likely affected the room pressure controllability more than they might affect in reality, because the controller settings are optimal for the nominal reference case values. Moreover, this has resulted in not being able to investigate the effect of room volume, because the PID-settings must be configured manually for every room volume, and hence, the PID-configuration inaccuracy outnumbered the effect of the room volume. Hence, in future research, it is recommended to investigate the possibility to include automatic PID-controller tuning.

The sensitivity analysis revealed that the control system and actuator properties do have a large impact, and therefore, should be chosen carefully to control the room pressure with sufficient accuracy within airtight cleanrooms. The main conclusions are as follows:

- With no leakage or overflow, the room pressure is uncontrollable, so a leakage really is a requirement. Hence, the controllability improves with increasing shell leakage which is the largest with low overflow rates. With higher overflow rates, the effect of increasing the shell leakage on the controllability is reduced. Moreover, with large overflow rates, active room pressure control is not required anymore.
- Both scenarios of the flow pressure cascade show a significant room pressure controllability improvement with increasing overflow rates. Next to that, the scenario where the total supply flow rate (mechanical and overflow) is kept constant reduces the

energy consumption. This scenario does achieve better room controllability than the scenario where only the mechanical supply flowrate is kept constant.

- The room pressure controllability may also be improved by removing the controller dead band and pressure sensor damping, although this may result in a lowered actuator lifetime.

Introducing a flow/pressure cascade with substantial overflow flowrate seems to be a good method to improve the room pressure controllability of airtight cleanrooms, as long as this can be united with the contamination control principles in the case it must be applied to.

5 REFERENCES

ABN Cleanroom Technology. (2020). *5 Forces That Drive Energy Efficiency in Pre-Engineered*. https://www.abn-cleanroomtechnology.com/uploads/files/Whitepaper-5-forces-that-drive-energy-efficiency-in-modular-cleanroom-design.05.pdf

Belimo. (2020). Actuator Applications Guide for heating, ventilation, and air conditioning.

Belimo. (2021a). Technical data sheet NMQ24A-MF NMQ24A-MF.

Belimo. (2021b). VAV-compact MOD product information.

Gassmann, E. (2014). Pressure-sensor fundamentals: Interpreting accuracy and error. *Chemical Engineering Progress*, *110*(6), 37–45.

Instrument Zero and Span Calibration - Instrumentation Tools. Retrieved January 19, 2022, from https://instrumentationtools.com/instrument-calibration/

ISO. (2019). ISO 14644-16 Cleanrooms and associated controlled environments | Energy efficiency in cleanrooms and separative devices. 13.

ISO. (2021). DRAFT INTERNATIONAL STANDARD ISO / DIS 14644-4 Cleanrooms and associated controlled environments — Part 4: Design, construction and start-up.

R&D world online. (2012). *Why Do Cleanrooms Fail to Meet Owners' Expectations?* https://www.rdworldonline.com/why-do-cleanrooms-fail-to-meet-owners-expectations/

Saurwalt, F. W. (2018). The Cleanroom zoning, the challenge of pressure differential and flow.

Sentra. (2018). Model 267 data sheet.

Ti-soft. (2017). *TiSoft - HeatingDesign Release 17.1.3*. https://www.ti-soft.com/en/products/software/heatingdesign/releasehistory/17_1_3

Trox. (2019a). BM0 Product data sheet.

Trox. (2019b). *TVR VAV-regelaar*.

van den Brink, A. H. T. M., & van Schijndel, A. W. M. (2012). Improved control of the pressure in a cleanroom environment. *Building Simulation*, *5*(1), 61–72.

VCCN. (2018). *VCCN richtlijn 10*. VCCN.

Wishart, A. (2018). *IdeadWhat! -why you need to be aware of integral deadband | LinkedIn*. https://www.linkedin.com/pulse/ideadwhat-why-you-need-aware-integral-deadband-alex/

Xu, Z. (2014). Characteristics of Air Filters. In *Fundamentals of Air Cleaning Technology and Its Application in Cleanrooms* (pp. 185–265). Springer Berlin Heidelberg.